


Spring 4-2015

## Synthesis of Potential Phosphorus-Nitrogen Containing Flame Retardants

Colin Kloock  
*University of Dayton*

Follow this and additional works at: [https://ecommons.udayton.edu/uhp\\_theses](https://ecommons.udayton.edu/uhp_theses)

 Part of the [Chemistry Commons](#)

---

### eCommons Citation

Kloock, Colin, "Synthesis of Potential Phosphorus-Nitrogen Containing Flame Retardants" (2015). *Honors Theses*. 71.

[https://ecommons.udayton.edu/uhp\\_theses/71](https://ecommons.udayton.edu/uhp_theses/71)

This Honors Thesis is brought to you for free and open access by the University Honors Program at eCommons. It has been accepted for inclusion in Honors Theses by an authorized administrator of eCommons. For more information, please contact [frice1@udayton.edu](mailto:frice1@udayton.edu), [mschlengen1@udayton.edu](mailto:mschlengen1@udayton.edu).

# **Synthesis of Potential Phosphorus- Nitrogen Containing Flame Retardants**



Honors Thesis

Colin Kloock

Department: Chemistry

Advisor: Vladimir Benin, Ph.D.

April 2015

# Synthesis of Potential Phosphorus-Nitrogen Containing Flame Retardants

Honors Thesis

Colin Kloock

Department: Chemistry

Advisor: Vladimir Benin, Ph.D.

April 2015

## Abstract

Production of extremely efficient flame retardants is ideal because, in many instances, the amount of flame retardants that are added to pre-production to the mixture are so large that they can have an effect on the physical properties of the material. In addition, these types of polymers, when added during production, are homogenously mixed throughout the mixture which means not only uniform distribution and therefore function, but a less concentration of the retardants need to be used. Using Phosphorus-Nitrogen containing flame retardants in mixtures can have two means by which they function. First is the ability of P-N compounds to crosslink or co-polymerize within the material at high temperatures such that it resembles a mesh. As temperatures increase, the amount of cross-bonding between the added flame retardants increases as well. In addition, the formation of phosphoryl radicals upon heating can interrupt one of the pathways by which combustion can occur, as it too involves free radicals. This is done by effectively removing hydroxyl radicals from the combustion process.

## Acknowledgements

I would like to thank the University of Dayton's Chemistry and the University Honors Program for giving me the amazing opportunity and resources to further myself and the field of chemistry. Without the guidance, mentorship, or time that Dr. Vladimir Benin has contributed to both myself and the project, this most certainly would not have been possible. Finally, to all of my professors, friends, and family that have given me support throughout the entire process and kept pushing me to the end.



## Table of Contents

Abstract	Title Page
Introduction	1
Results and Discussion	7
Experimental	15
Conclusion and Future Directions	20
Bibliography	21

## Introduction:

The field of synthetic flame retardants that can be incorporated into the production of materials is growing because the need for safe, but highly effective flame retardants is also growing. Typically, flame retardants are simply blended into polymeric mixtures during production, but the downside is the concentration of flame retardants needed. Some formulations actually require up to 30% of the mixture to be the flame retardant, which can have adverse effects such as altering both the physical and mechanical structure of the material. To deter this, more efficient flame retardants are being synthesized allowing for lower concentrations of the flame retardant while still producing comparable flame retardant effect. During combustion, apart from the fatalities owed to the fire, some flame retardants can evolve toxic gases that can be just as fatal or have long-lasting effects. To produce not only efficient, but safe flame retardants that can be incorporated during production is ideal and necessary.

The market for flame retardants is relatively high and measures about 11%, \$4.2 billion, of a \$36.2 billion plastic additives market. The major flame retardant families are bromine-based, phosphorus-based, inorganic-based, chlorine-based, and melamine as illustrated in Figure 1.

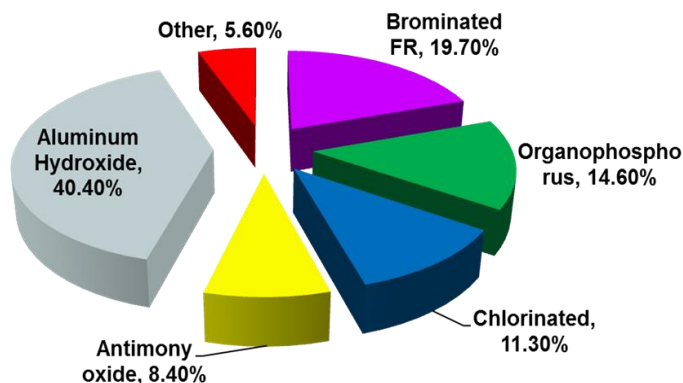


**Figure 1.** Families of current flame retardants and their respective share of the market

This project focused on phosphorus-based flame retardants and their ability to effectively inhibit combustion. Specifically, the goal was to prepare and test structures that would act as reactive flame retardants. The traditionally used, additive flame retardants are evenly mixed into the polymer during foam manufacture, but are not chemically bonded to the polymer. They are inexpensive and relatively easy to add and mix; however, there is a potential to leach out which poses environmental threats and a decrease in protection over time. Reactive flame retardants, the focus of this research, actually co-polymerize and covalently bond into the polymer chain during manufacture. Because of that, reactive flame retardants cannot leach out of foam and can provide flame retardant chemistry directly to polymer backbone as it decomposes. On the other hand, reactive flame retardants can change polymerization kinetics, alter mechanical properties of the polymer, and can be more expensive.

Flame retardant mechanisms have many facets. One of the more common mechanisms of action is the creation of a mesh over the material that aids in the retarding of flame production. The goal of this project is the synthesis of phosphorus-nitrogen flame retardants through reactions of nitrogen containing compounds with phosphoryl chlorides. The primary goal of flame retardants that are incorporated into either pre-production or added post-production, are to inhibit or delay the combustion of the material. Delayed combustion is important because it essentially is an added safety measure to the product -- more time to combust means more time to escape if the chance of combustion were plausible. The goal of this project is to create phosphorus-nitrogen containing compounds that can be incorporated into polymeric mixtures to maximize flame retardancy, but minimize the amount needed. The potential incorporation of the

flame retardant into a polymer backbone such as urethane is possible. The production of urethane is seen in figure 2. Figure 3 is comprised of a few commercially P-based flame retardants for polyurethane.

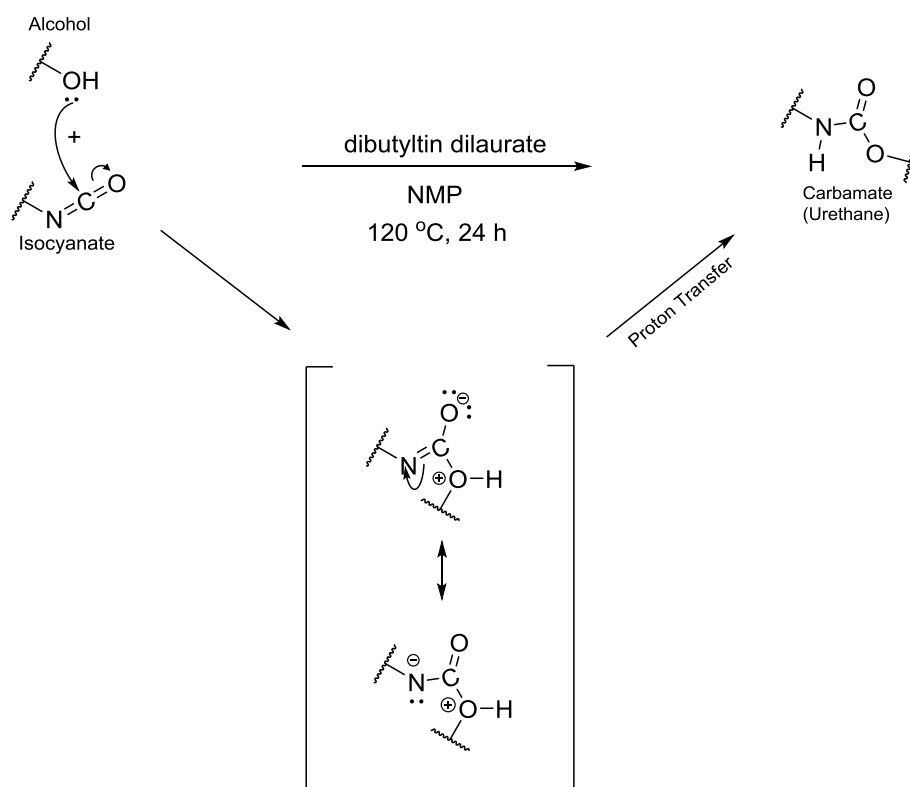


**Figure 2.** Suggested pathway of urethane formation

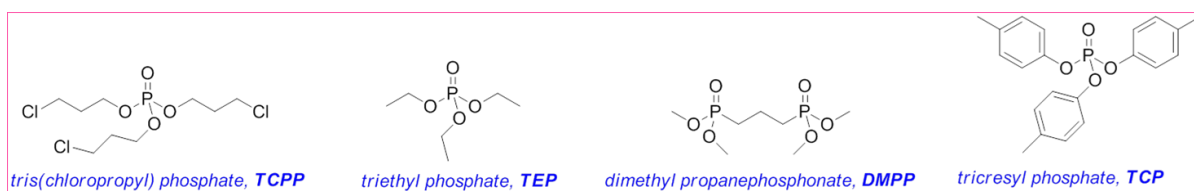


**Figure 3.** Common commercial P-based FR for polyurethanes

Organic synthesis of these phosphorus-nitrogen containing compounds is done and then the phosphorus-nitrogen compounds are then oxidized. The generation of an N-N double bond increases bond conjugation and shifts the absorbance of the molecule into in visible light range to produce an orange color. The general reactions to produce the

phosphorus-nitrogen compounds and subsequent phosphorus-nitrogen compounds are seen in Figure 4 and Figure 5.

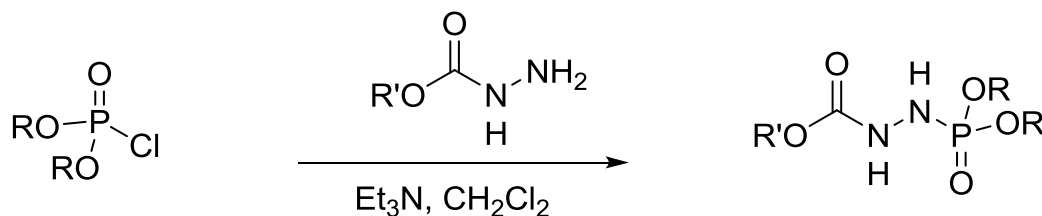


**Figure 4** Illustrates the general nucleophilic substitution reaction at phosphorus, with a carbazate nucleophile

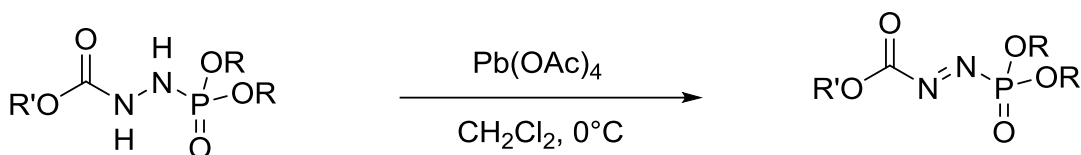


**Figure 5** The oxidation of phosphorus-nitrogen flame retardant to azophosphonate by use of lead(IV) acetate

There are two different processes and phases that accompany the flame retardancy: the gas phase and the condensed phase. Figure 6 shows the multiple different routes the process of combustion can take. Within the gas phase, the production of combustible volatile products is one of the main ways a flame is produced. The increase in N-N double bonds is likely to produce greater likelihood for the generation of phosphoryl radicals at elevated temperatures, which would be beneficial both from the perspective of fire-retardancy and the ability to co-polymerize in radical processes.



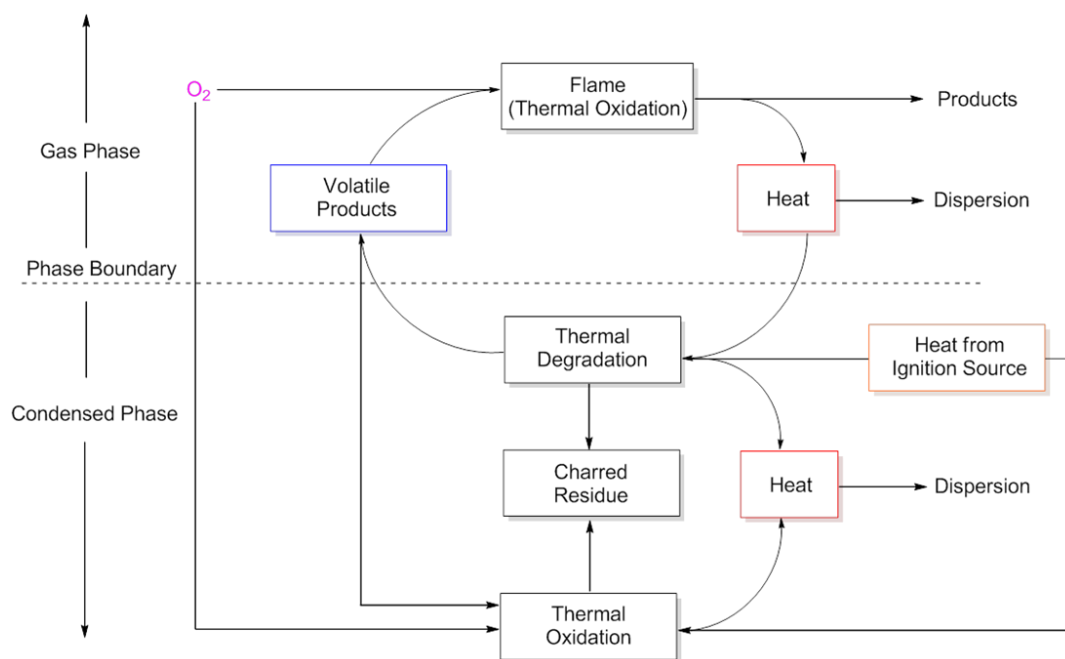


**Figure 6.** The two phases of combustion of a polymeric material

Phosphorus compounds are commonly known to induce char formation with a plethora of heteroatom-containing polymers (polymers with either oxygen or nitrogen in their structure). This occurs during heating where the formation of extensive phosphorus-oxygen or phosphorus-nitrogen networks yielding what is known as thermosets that are difficult to melt. This thermoset protects against the fire for the polymer beneath the thermoset. Figure 7 illustrates a suggested pathway of char formation.

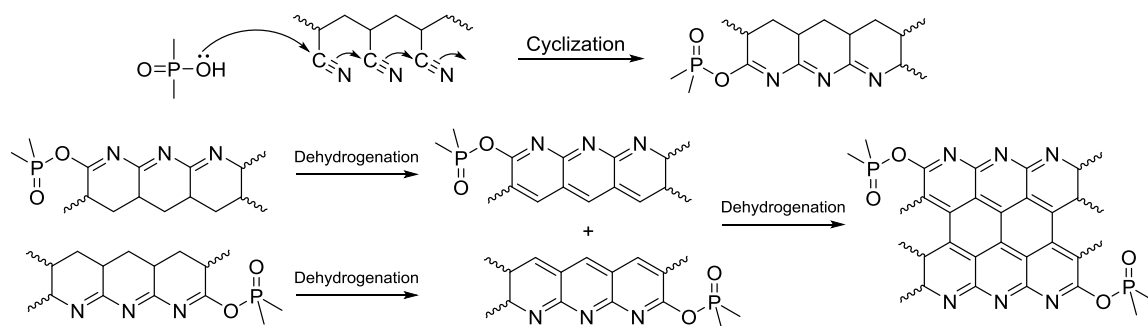


**Figure 7.** Suggested pathway for the formation of char in a polymer sample containing a phosphorous-based flame retardant

Char formation can occur in the condensed phase of combustion. The process is the result of several factors: Faster decomposition in the presence of P-flame retardant, removal of volatiles, and cross-linking. Within the gas phase, hydrogen and hydroxyl radicals are replaced by less effective phosphoryl radicals or are rendered harmless by radical recombination. Figure 8 is the general pathway by which the phosphoric acid functionalities interact with the polymer in the process of combustion. The result is the regeneration of an isocyanate compound and an alcohol. The phosphoric acid then combines with the isocyanate compound to form cross links.

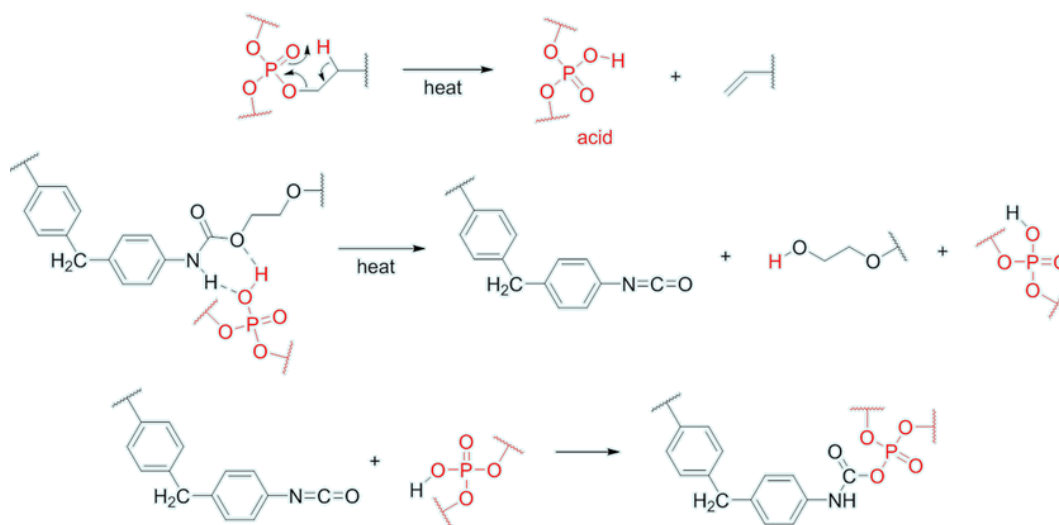


**Figure 8.** The action and mechanism of phosphorus-based flame retardant incorporation

Upon heating, the oxidized phosphorus-nitrogen containing flame retardant, which is now an azophosphonate, will begin to break down. The process by which this happens is illustrated in Figure 8 and begins with either the *cis* or *trans* conformation of the azophosphonate as many double bond containing compounds interconvert upon heating.

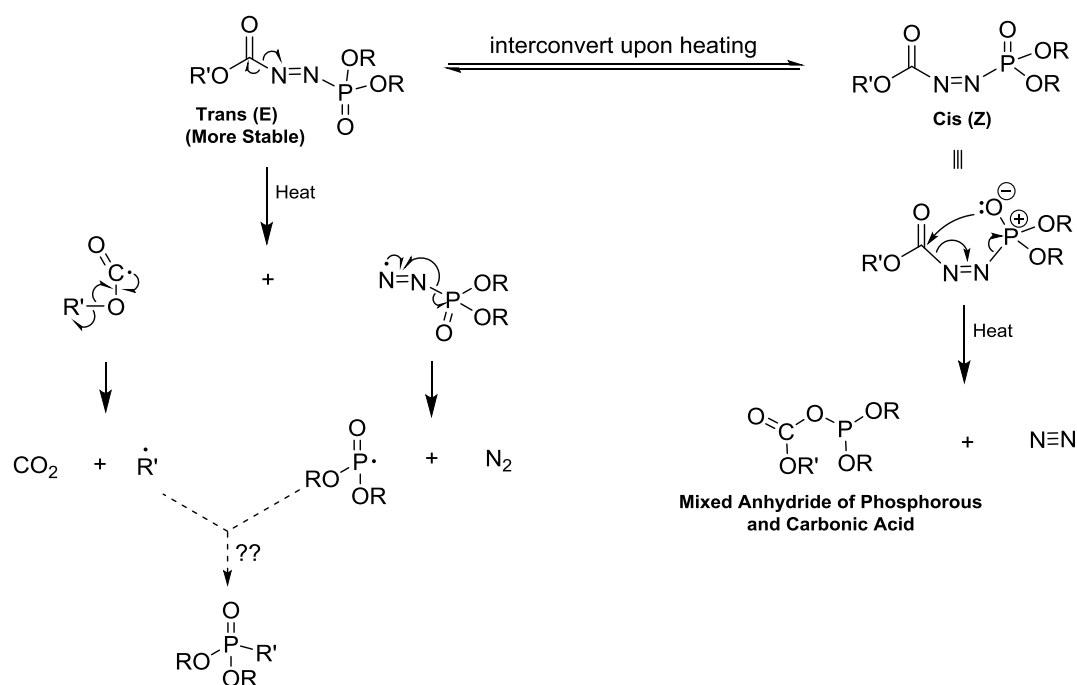


**Figure 8.** Proposed decomposition of an azophosphonate

The generation of the phosphoryl radical is highly desired because it can seek out the hydroxyl radicals, which are key participants in several combustion reactions as mentioned previously. A driving force for this reaction to proceed is the production of elemental nitrogen and carbon dioxide, two very stable compounds.

## Results and Discussions:

### Synthesis of Hydrazophosphonates:

Synthesis of hydrazophosphonate flame retardants was achieved by general nucleophilic substitution reactions at phosphorus with a carbazate nucleophile. Two different carbazate nucleophiles were used: ethyl carbazate and t-butyl carbazate. The

nucleophilic substitution beings by nucleophilic attack by the nitrogen at the phosphorus center of the phosphoryl chloride as seen in Figure 9 and 10.

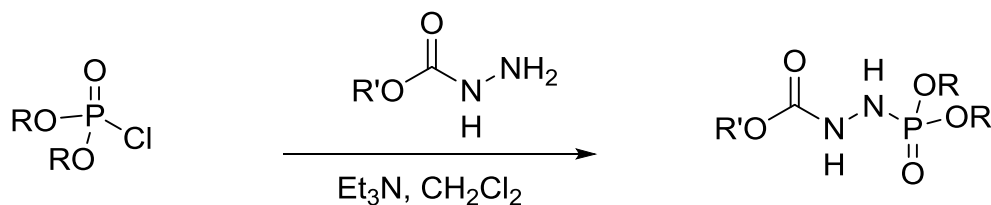


**Figure 9.** General scheme of nucleophilic substitution reactions using a carbazate nucleophile

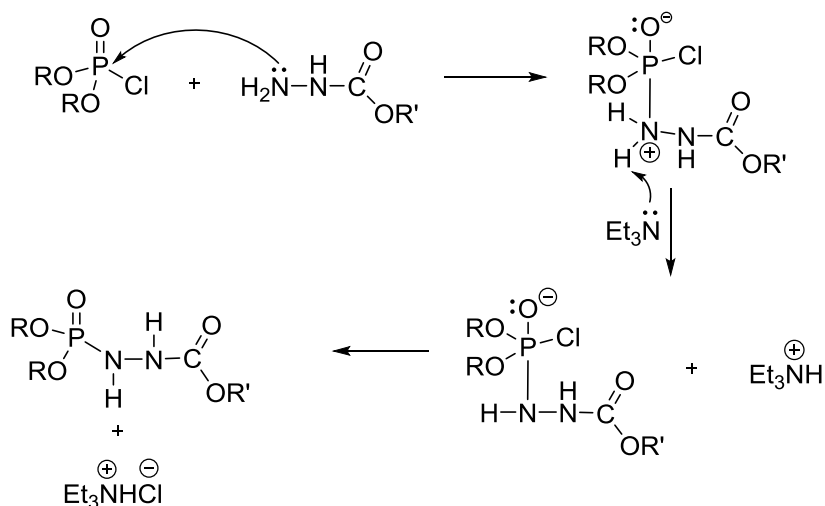


**Figure 10.** Mechanism of nucleophilic substitution reactions at phosphorus.

### Reactions with Ethyl Carbazate:

The following 3 reaction schemes utilized an ethyl carbazate nucleophile and are conveyed in Figure 11. Initial synthesis began with an acyclic phosphoryl chloride reacted with ethyl carbazate and triethylamine in methylene chloride to yield the corresponding hydrazophosphonate. Subsequent nucleophilic reactions used a monocyclic and then bicyclic reagent as opposed to the acyclic compound.

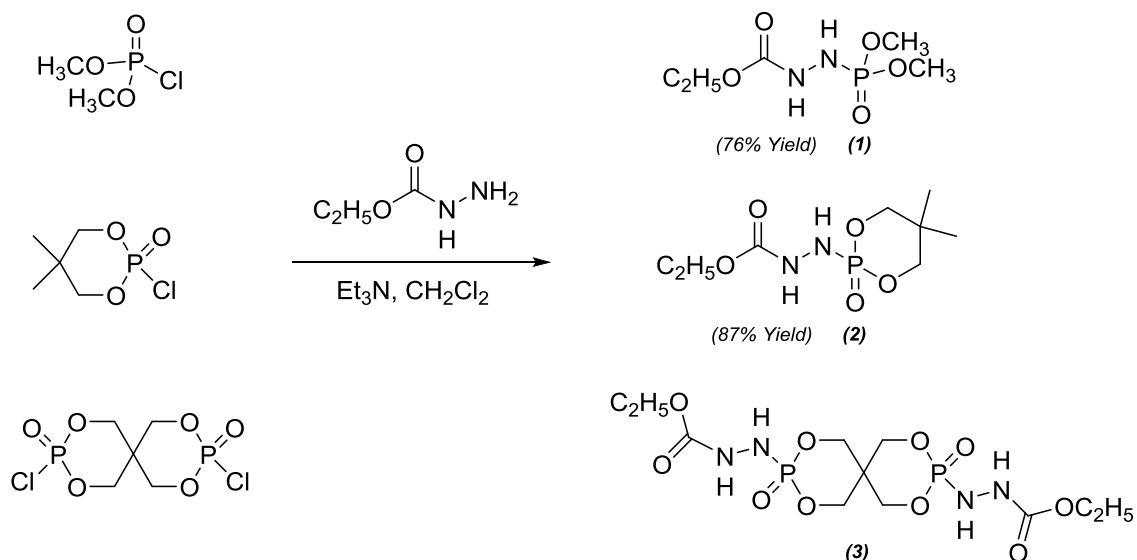


**Figure 11.** Nucleophilic substitution reactions by ethyl carbazate at phosphorus to produce subsequent hydrazophosphonates

#### Reactions with t-Butyl Carbazate:

Similar to the previous ethyl carbazate-based nucleophilic reactions, the subsequent two reactions utilized t-Butyl carbazate as the nucleophile. Initially, a monocyclic phosphoryl chloride was reacted with t-Butyl carbazate and triethylamine in methylene chloride to yield the corresponding monocyclic hydrazophosphonates. Figure 12 depicts this synthesis of a hydrazophosphonate using t-Butyl as a nucleophile and corresponds to the mechanism given in Figure 10.

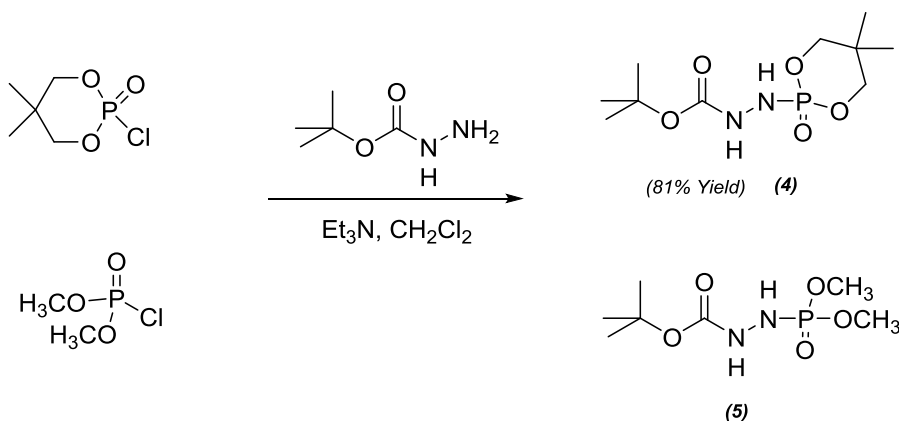


**Figure 12** is a schematic representation of the t-butyl carbazate nucleophile reactions.

### Oxidation of Hydrazophosphonates to Azophosphonates:

The hydrazophosphonates synthesized were subjected to general oxidation by lead(IV)acetate to yield azophosphonates. Figure 13 shows the schematic representation of such oxidation and Figure 14 illustrates the mechanism of oxidation. The mechanism of oxidation begins with nucleophilic attack on the lead center by nitrogen. After rearrangement, the desired azophosphonate in addition to Lead(II)Acetate and acetic acid.

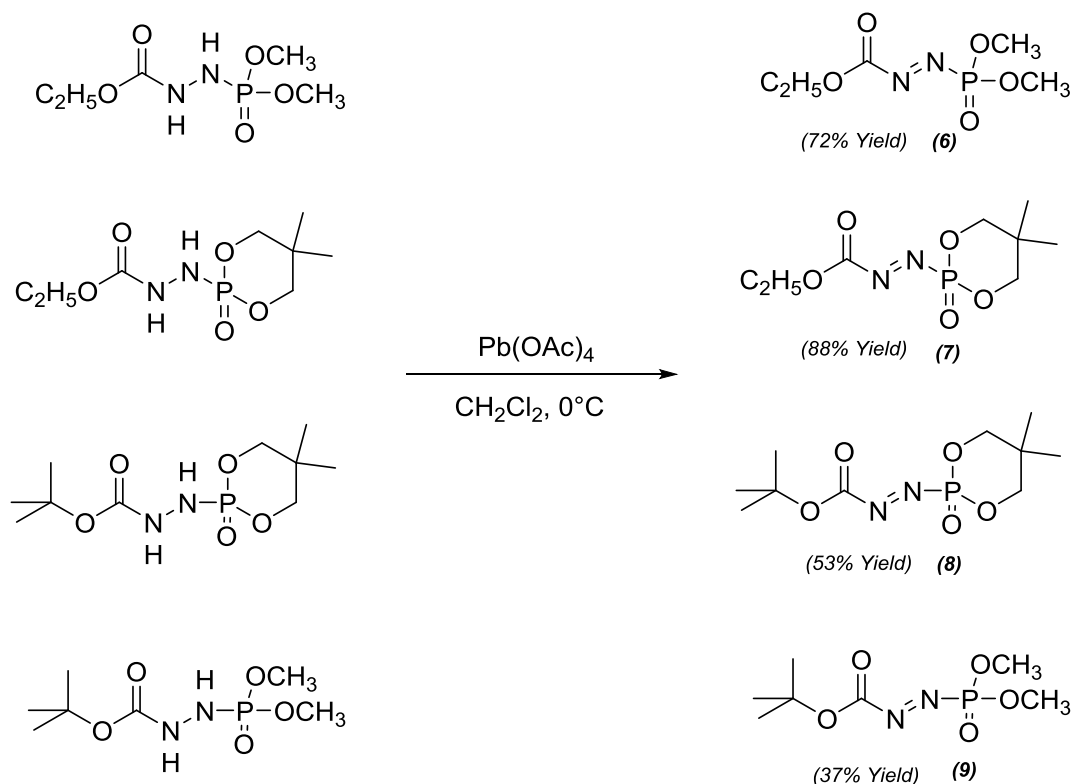


**Figure 13.** Oxidation of hydrazophosphonates to azophosphonates by lead(IV)acetate

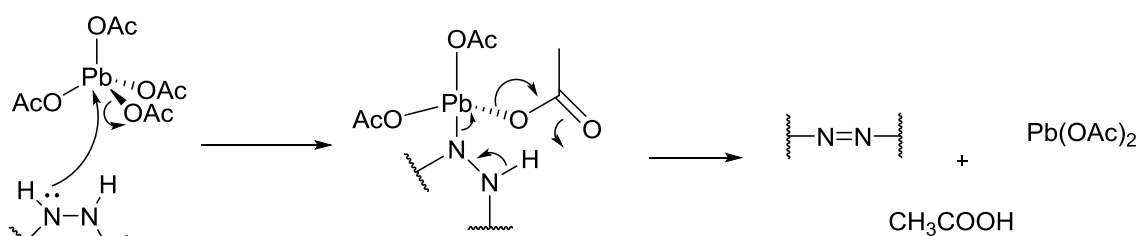


**Figure 14.** The mechanism of oxidation of the hydrazophosphonate to an azophosphonate by Lead(IV)Acetate

## Thermal Decomposition of Azophosphonates:

### Protocol for Kinetic Studies:

- Prepare an NMR sample of studied azophosphonate in DMSO- $d_6$
- Run  $^1\text{H}$  NMR spectrum at ambient temperature. Integrate signals relative to signal of the solvent.
- Heat sample for a set time interval, then measure  $^1\text{H}$  NMR spectrum and integrate relative to signal of the solvent. Repeat and follow disappearance of the signals of the starting material
- Choose a specific signal of the starting material and calculate ratios of integral for that signal at certain time vs. integral for the same signal before heating (this corresponds to ratio of concentrations:  $[A]/[A_0]$ )
- Plot  $\ln([A]/[A_0])$  vs. time

To prepare an NMR sample, the desired azophosphonate was obtained and using a glass pipette and bulb, a small portion of the compound was dissolved in the solvent: DMSO- $d_6$  or  $\text{CDCl}_3$ . Once the compound is dissolved in the solvent, the solution is pipetted into the NMR tube to be studied. To perform variable temperature NMR studies, it was necessary to take an ambient, starting temperature sample and then heat the sample in the NMR tube in an oil bath of desired temperature. After the allotted time had past while the tube was submerged, it was dried and hexanes were used to ensure no oil was present. Next, the NMR sample was taken to be studied. After constructing a rate plot, the rate constants for decomposition are known and can be used to construct an Eyring plot where  $\ln(k/T)$  vs.  $1/T$  are plotted. After plotting these points,

rearrangement of the Eyring equation to resemble that of slope-intercept form allows the derivation of the entropy and enthalpy of decomposition as seen in the set of equations below.

$$\begin{aligned}
 k &= \frac{k_b T}{h} e^{\frac{-\Delta H^\ddagger}{RT}} * e^{\frac{\Delta S^\ddagger}{R}} \\
 \frac{k}{T} &= \frac{k_b}{h} e^{\frac{-\Delta H^\ddagger}{RT}} * e^{\frac{\Delta S^\ddagger}{R}} \\
 \frac{k}{T} &= \frac{k_b}{h} e^{\frac{\Delta S^\ddagger}{R}} * e^{-\Delta H^\ddagger} \\
 \ln\left(\frac{k}{T}\right) &= \ln\left(\frac{k_b}{h}\right) + \frac{\Delta S^\ddagger}{R} - \frac{\Delta H^\ddagger}{R} * \frac{1}{T} \\
 Y &= b + (-mx)
 \end{aligned}$$

**Figure 14.** The derivation of the Eyring equation

The kinetic studies of the monocyclic azophosphonate were extensive and followed the protocol listed previously. A rate plot was constructed with four different rates of decomposition for four different temperatures: 353K, 379K, 393K, and 413K as seen in Figure 15.



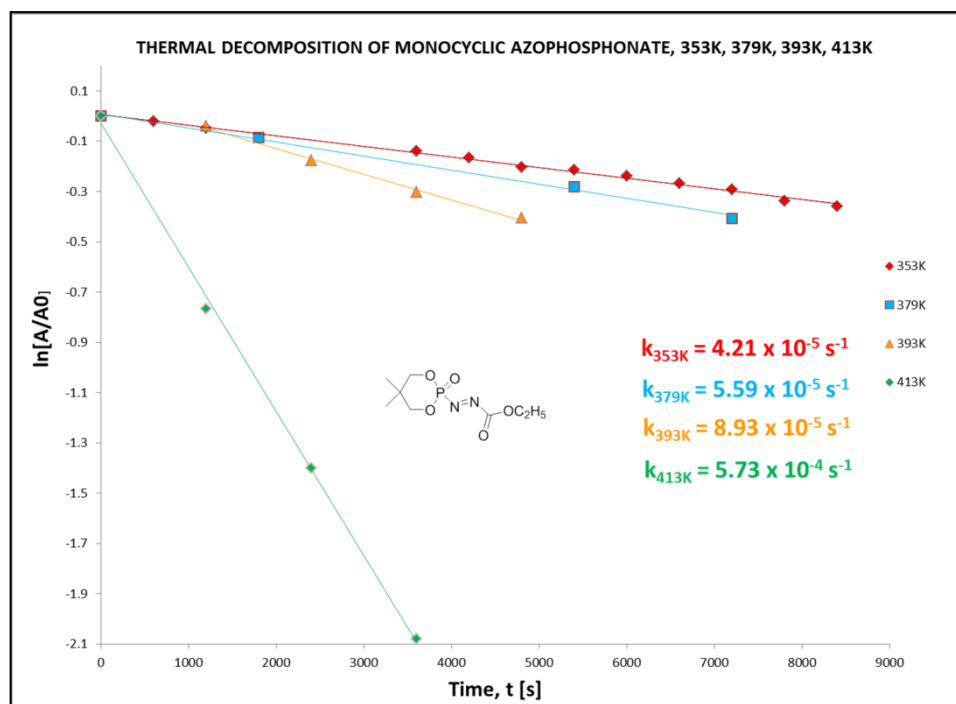


**Figure 15.** Rate plots for the thermal decomposition of the monocyclic azophosphonate.

Now that a set of rate constants have been determined, plotting  $\ln(k/T)$  vs.  $1/T$  allows for the derivation of the enthalpy and entropy of decomposition. This is seen in Figure 16 where an Eyring plot of the decomposition of the monocyclic azophosphonate has been constructed.

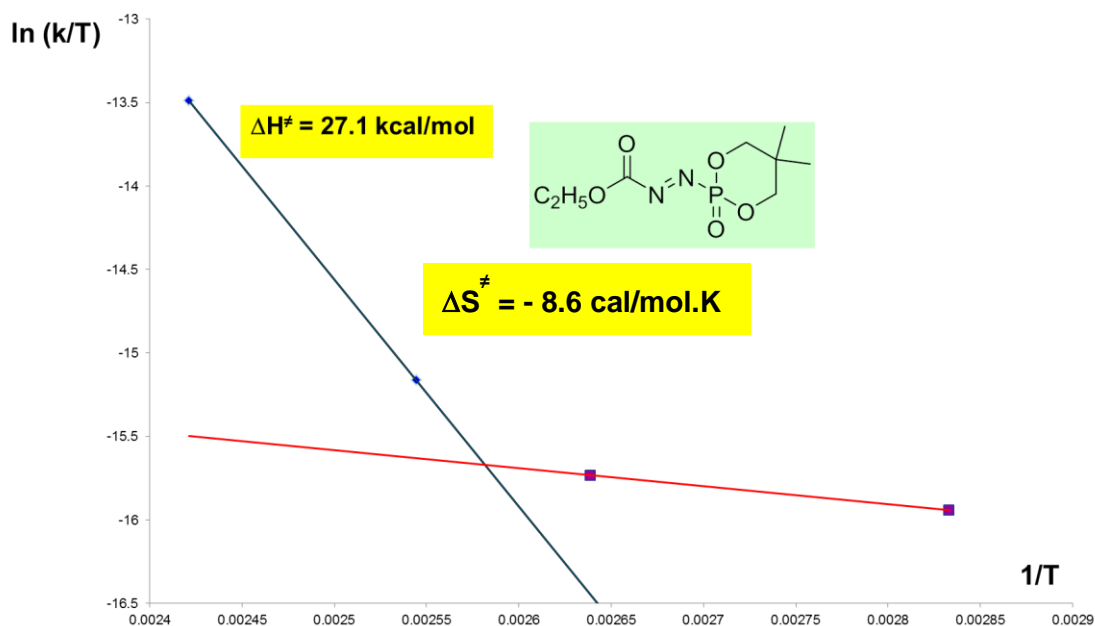


**Figure 16.** Eyring plot for the thermal decomposition of the monocyclic azophosphonate

The curvature of the Eyring plot suggests a potential change in mechanism for the decomposition of azophosphonates. Further investigation is necessary to clarify the details of the decomposition mechanism.

Calculations are being conducted to gain further insight into the mechanism of thermal decomposition and structure of the corresponding transition states.

Calculations also yield relevant thermodynamic values. Part of the potential energy profile for the thermal decomposition of an acyclic azophosphonate is shown below, in Figure 17.

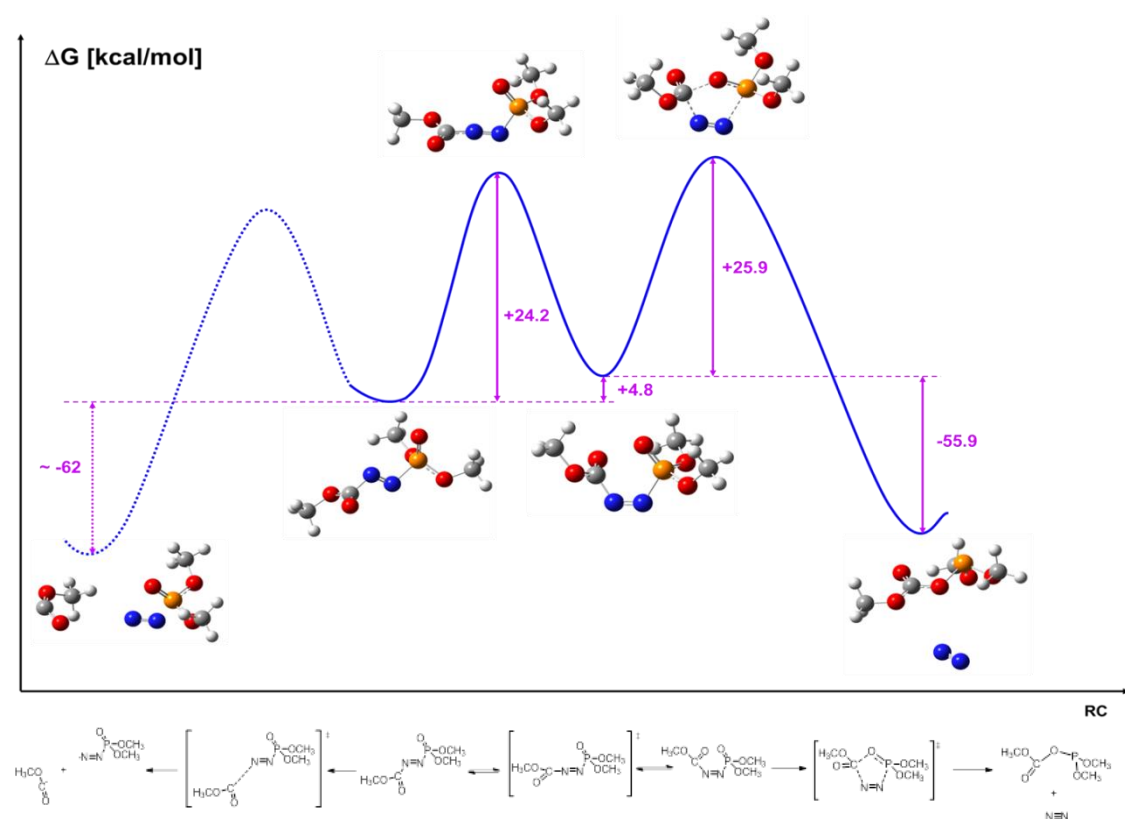


**Figure 17.** The proposed reaction coordinate diagram of decomposition with accompanying Gibbs' free energy values

## Experimental:

**Ethyl 2-(dimethoxyphosphoryl)hydrazine-1-carboxylate (1)** A mixture of dimethyl chlorophosphate (1.39g, 9.6 mmol, 1.04mL), ethyl carbazate (1.00g, 9.6 mmol), and triethylamine (0.97g, 9.6 mmol, 1.34 mL) were combined in a round bottom flask with methylene chloride (10 mL) and stirred for 18 h at 0 °C under nitrogen. The resultant mixture was vacuum filtered where the solid precipitate was discarded and the mother liquor was left to evaporate. The evaporated mother liquor was filtered twice using silica gel through an elution column by ethyl acetate and a third filtration used a 10:1 ethyl acetate:methanol solution. The three elutions were combined in a round

bottom flask and then roto-vapped to yield the ethyl 2-(dimethoxyphosphoryl)hydrazine-1-carboxylate (76% yield).  $^1\text{H}$  NMR ( $\text{CDCl}_3$ )  $\delta$  1.26 (t,  $J = 7.1$  Hz, 3H), 3.81 (d,  $J = 11.2$  Hz, 6H), 4.18 (q,  $J = 7.1$  Hz, 2H), 5.64 (d,  $J = 32.9$  Hz, 1H), 6.65 (s, 1H).  $^{13}\text{C}$  NMR ( $\text{CDCl}_3$ )  $\delta$  14.4, 53.8(d,  $J = 5.2$  Hz), 61.9, 157.0;  $^{31}\text{P}$  7.6; Anal Calcd. For  $\text{C}_5\text{H}_{13}\text{O}_5\text{N}_2\text{P}$ : C, 28.31; H, 6.18; N, 13.21. Found: C 28.01; H, 6.23; N, 13.38.

**Ethyl 2-(5,5-dimethyl-2-oxido-1,3,2-dioxaphosphinan-2-yl)hydrazine-1-carboxylate (2)** A mixture of 2-chloro-5,5-dimethyl-1,3,2-dioxaphosphinane 2-oxide (1.78g, 9.6 mmol), ethyl carbazate (1.00g, 9.6 mmol), and triethylamine (0.98g, 9.6 mmol, 1.34 mL) were combined in a round bottom flask with methylene chloride (10 mL) and stirred for 18 h at 0 °C under nitrogen. After 18 h of stirring, the mixture was then stirred at 80 °C for 4 h with a condensing attachment under nitrogen. The mother liquor was filtered three using silica gel through an elution column by ethyl acetate. The three elutions were combined in a round bottom flask and then roto-vapped to yield the ethyl 2-(5,5-dimethyl-2-oxido-1,3,2-dioxaphosphinan-2-yl)hydrazine-1-carboxylate (87% yield).  $^1\text{H}$  NMR ( $\text{CDCl}_3$ )  $\delta$  1.07 (d,  $J = 20.7$  Hz, 6H), 1.26 (t,  $J = 7.1$  Hz, 3H), 4.17 (m, 6H), 5.65 (d,  $J = 31.35$  Hz, 2H), 6.85 (s, 1H).  $^{13}\text{C}$  NMR ( $\text{CDCl}_3$ )  $\delta$  14.4, 21.09 (d,  $J = 33.45$  Hz), 32.0 (d,  $J = 6.075$ ), 62.0, 77.6 (d,  $J = 6.0$  Hz), 157.0 (d,  $J = 2.25$ );  $^{31}\text{P}$  20.98; Anal Calcd. for  $\text{C}_8\text{H}_{17}\text{O}_5\text{N}_2\text{P}$ : C, 38.10; H, 6.79; N, 11.11. Found: C 35.39; H, 6.67; N, 10.42.

**Diethyl 2,2'-(3,9-dioxido-2,4,8,10-tetraoxa-3,9-diphosphaspiro[5.5]undecane-3,9-diyl)bis(hydrazine-1-carboxylate) (3)** A mixture of 3,9-dichloro-2,4,8,10-tetraoxa-3,9-diphosphaspiro[5.5]undecane 3,9-dioxide (1.425g, 4.8 mmol) and ethyl carbazate (1.00g, 9.6 mmol) were combined in a round bottom flask with pyridine (5 mL) as

solvent and stirred for 24 h at room temperature under nitrogen. Diethyl ether (100 mL) was added to the mixture and a white precipitate formed. 1.5M HCl (40 mL) was added and two distinct layers formed. The layers were separated using a separatory funnel. Clear top layer was combined with MgSO<sub>4</sub> to dry the solution. The resulting dried solution was filtered using gravity filtration, but no product was obtained upon roto-vapping. The second, cloudy layer, was combined with methylene chloride (10 mL) and NaCl. The solution was separated using a separatory funnel and the cloudy layer was once again filtered using gravity filtration. The resulting mixture did not yield any product after being roto-vapped. Therefore, the synthesis of Diethyl 2,2'-(3,9-dioxido-2,4,8,10-tetraoxa-3,9-diphosphaspiro[5.5]undecane-3,9-diyl)bis(hydrazine-1-carboxylate) was unsuccessful (0% yield). <sup>1</sup>H NMR (CDCl<sub>3</sub>) δ 1.24 (t, J = 371.58 Hz, 3H), 3.79 (d, J = 11.21 Hz, 6H), 4.15 (q, J = 7.11 Hz 2H), 5.89 (d, J = 33.32 Hz, 2H), 6.89 (s, 1H). <sup>13</sup>C NMR (CDCl<sub>3</sub>) δ 14.4, 53.77(d, J = 5.175 Hz), 61.807, 77.0 (t, J = 31.8 Hz), 157.0; <sup>31</sup>P 7.83; Anal Calcd. For C<sub>11</sub>H<sub>22</sub>O<sub>10</sub>N<sub>4</sub>P<sub>2</sub>: C, 52.06; H, 5.52; N, 6.39. Found: C 52.04; H, 5.50; N, 6.44.

**t-Butyl 2-(5,5-dimethyl-2-oxido-1,3,2-dioxaphosphinan-2-yl)hydrazine-1-carboxylate (4)** A mixture of 2-chloro-5,5-dimethyl-1,3,2-dioxaphosphinane 2-oxide (1.39g, 7.57 mmol), t-butyl carbazate (1.00g, 7.57 mmol), and triethylamine (0.76g, 7.57 mmol, 1.05 mL) were combined in a round bottom flask with chloroform (20 mL) and stirred for 24 h at room temperature under nitrogen. After 24 h of stirring, the mixture was then stirred at 70 °C for 4 h with a condensing attachment under nitrogen. The mother liquor was filtered three using silica gel through an elution column by ethyl acetate. The three elutions were combined in a round bottom flask and then roto-vapped

to yield the t-butyl 2-(5,5-dimethyl-2-oxido-1,3,2-dioxaphosphinan-2-yl)hydrazine-1-carboxylate (81% yield).

**t-Butyl 2-(dimethoxyphosphoryl)hydrazine-1-carboxylate (5)** A mixture of dimethyl chlorophosphate (1.81g, 7.57 mmol), t-butyl carbazate (1.00g, 7.57 mmol), and triethylamine (0.76g, 7.57 mmol, 1.05 mL) were combined in a round bottom flask with chloroform (20 mL) and stirred for 24 h at room temperature under nitrogen. After 24 h of stirring, the mixture was then stirred at 70 °C for 4 h with a condensing attachment under nitrogen. The mother liquor was filtered three using silica gel through an elution column by ethyl acetate. The three elutions were combined in a round bottom flask and then rotovapped to yield the t-butyl 2-(dimethoxyphosphoryl)hydrazine-1-carboxylate (81% yield).  $^1\text{H}$  NMR ( $\text{CDCl}_3$ )  $\delta$  1.43 (s, 10H), 3.79 (q,  $J = 59.0$  Hz, 5H), 5.64 (d,  $J = 33.0$  Hz, 1H), 6.50 (s, 1H).  $^{13}\text{C}$  NMR ( $\text{CDCl}_3$ )  $\delta$  28.11 (d,  $J = 3.9$  Hz), 53.73 (d,  $J = 5.25$  Hz), 77.0 (t,  $J = 31.8$  Hz), 81.1, 156.0;  $^{31}\text{P}$  7.91; Anal Calcd. For  $\text{C}_7\text{H}_{17}\text{O}_5\text{N}_2\text{P}_1$ : C, 35.00; H, 7.13; N, 11.66. Found: C 35.53; H, 6.88; N, 12.25.

**Ethyl (E)-2-(dimethoxyphosphoryl)diazene-1-carboxylate (6)** A mixture of ethyl 2-(dimethoxyphosphoryl)hydrazine-1-carboxylate (0.4g, 1.88 mmol) and lead(IV)acetate (1.016g, 2.229 mmol) in methylene chloride (30 mL) were stirred at 0 °C for 0.5 h. The resultant orange mixture was washed three times in  $\text{H}_2\text{O}$  in a separatory funnel. The clear, orange, bottom layer was dried using  $\text{MgSO}_4$  and then subjected to gravity filtration. The filtered solution was then eluted through silica gel by a 2:1 ethyl acetate:hexane solution. The final orange solution was roto-vapped to yield a viscous orange product: the ethyl (E)-2-(dimethoxyphosphoryl)diazene-1-carboxylate (72%

yield).  $^1\text{H}$  NMR ( $\text{DMSO-}d_6$ )  $\delta$  1.35 (t,  $J = 7.12$  Hz, 3H), 3.55 (d,  $J = 11$  Hz, 2H), 3.92 (d,  $J = 10.67$ , 6H), 4.49 (q,  $J = 7.10$  Hz, 2H).

**Ethyl (E)-2-(5,5-dimethyl-2-oxido-1,3,2-dioxaphosphinan-2-yl)diazene-1-carboxylate (7)** A mixture of ethyl 2-(5,5-dimethyl-2-oxido-1,3,2-dioxaphosphinan-2-yl)hydrazine-1-carboxylate (0.5522g, 2.36 mmol) and lead(IV)acetate (1.27g, 2.85 mmol) in methylene chloride (30 mL) were stirred at 0 °C for 0.5 h. The resultant orange mixture was washed three times in  $\text{H}_2\text{O}$  in a separatory funnel. The clear, orange, bottom layer was dried using  $\text{MgSO}_4$  and then subjected to gravity filtration. The filtered solution was then eluted through silica gel by a 2:1 ethyl acetate:hexane solution. The final orange solution was roto-vapped to yield a viscous orange product: the ethyl (E)-2-(5,5-dimethyl-2-oxido-1,3,2-dioxaphosphinan-2-yl)diazene-1-carboxylate (88% yield).  $^1\text{H}$  NMR ( $\text{DMSO-}d_6$ )  $\delta$  0.87 (s, 3H), 1.3 (s, 3H), 1.40 (t,  $J = 7.12$  Hz, 3H), 4.25 (m, 4H), 4.52 (q,  $J = 7.01$  Hz, 2H).

**t-Butyl (E)-2-(5,5-dimethyl-2-oxido-1,3,2-dioxaphosphinan-2-yl)diazene-1-carboxylate (8)** A mixture of tert-butyl 2-(5,5-dimethyl-2-oxido-1,3,2-dioxaphosphinan-2-yl)hydrazine-1-carboxylate (1.25g, 4.46 mmol) and lead(IV)acetate (2.39g, 5.35 mmol) in methylene chloride (30 mL) were stirred at 0 °C for 0.5 h. The resultant orange mixture was washed three times in  $\text{H}_2\text{O}$  in a separatory funnel. The clear, orange, bottom layer was dried using  $\text{MgSO}_4$  and then subjected to gravity filtration. The filtered solution was then eluted through silica gel by a 2:1 ethyl acetate:hexane solution. The final orange solution was roto-vapped to yield a viscous orange product: the tert-butyl (E)-2-(5,5-dimethyl-2-oxido-1,3,2-dioxaphosphinan-2-yl)diazene-1-carboxylate (53% yield).

**t-Butyl (E)-2-(dimethoxyphosphoryl)diazene-1-carboxylate (9)** A mixture of tert-butyl 2-(dimethoxyphosphoryl)hydrazine-1-carboxylate (0.5g, 2.08 mmol) and lead(IV)acetate (1.05g, 2.33 mmol) in methylene chloride (30 mL) were stirred at 0 °C for 0.5 h. The resultant orange mixture was washed three times in H<sub>2</sub>O in a separatory funnel. The clear, orange, bottom layer was dried using MgSO<sub>4</sub> and then subjected to gravity filtration. The filtered solution was then eluted through silica gel by a 2:1 ethyl acetate:hexane solution. The final orange solution was roto-vapped to yield a viscous orange product: the tert-butyl (E)-2-(dimethoxyphosphoryl)diazene-1-carboxylate (37% yield).

## Conclusion and Future Directions:

New hydrazophosphonates have been prepared and characterized by <sup>1</sup>H and <sup>13</sup>C NMR, and elemental analysis. The hydrazophosphonates were successfully oxidized and the resultant azophosphonates have been characterized using <sup>1</sup>H and <sup>13</sup>C NMR. Kinetic studies currently incomplete but rate plots at individual temperatures are linear. The curved Eyring plot may point out to a change of mechanism or interplay of competing pathways of decomposition. Complete characterization of hydrazo- and azophosphonates. Complete kinetic studies and derive activation parameters. Utilize azophosphonates in Diels-Alder type cycloaddition reactions. The last future plan is to react azophosphonates into polyurethanes and study their flammability.



## Bibliography

- Azzouz, R.; Fruit, C.; Bischoff, L.; Marsais, F. *J. Org. Chem.* 2008, 73, 1154 - 1157
- Chandrasekhar, M; Chandra, K. L.; Singh, V. K. *J. Org. Chem.* 2003, 68, 4039 – 4045
- Darrow, J. W.; Drueckhammer, D. G. *J. Org. Chem.* **1994**, 59, 2976 – 2985
- Das, S.; Misra, A. K.; Kumar, A.; Al Ghamdi, A. K.; Yadav, J. S. *Carbohydr. Res.* **2012**, 358, 7 – 11
- Georlette, P.; Simons, J.; Costa, L. “*Fire Retardancy of Polymeric Materials*” 2000, Marcel Dekker,
- Grand, A. F.; Wilkie, C. A., Eds., 1<sup>st</sup> Ed., pp. 245 - 285
- Joseph, Paul, and Svetlana Tretyakova-McNally. "Reactive Modifications of some Chain- and Step-Growth Polymers with Phosphorus-Containing Compounds: Effects on Flame Retardance? a Review." *Polymers for Advanced Technologies* 22.4 (2011): 395-406. Print.
- Khan, A. T.; Khan, M. M.; Adhikary, A. *Carbohydr. Res.* **2011**, 346, 673 – 677
- Kolodyazhnaya, A. O.; Kukhar, V. P.; Kolodyazhnyi, O. I. *Rus. J. Gen. Chem.* 2004, 74, 1945 - 1946
- Kumaraswamy, S.; Sentamizh Selvi, R.; Kumara Swamy, K. C. *Synthesis* 1997, 207 – 212
- Lu, S.-Y.; Hamerton, I. *Prog. Polym. Sci.* **2002**, 27, 1661 – 1712
- Merrer, Y.; Dureault, A.; Greck, C.; Micas-Languin, D.; Gravier, C.; Depezay, J.-C. *Heterocycles* 1987, 25, 541 - 548
- Shing, T. K. M.; Wong, W. F.; Ikeno, T.; Yamada, T. *Chem. Eur. J.* **2009**, 15, 2693 – 2707